Colloids and Surfaces A: Physicochemical and Engineering Aspects 700 (2024) 134773

Contents lists available at ScienceDirect

Colloids and Surfaces A: Physicochemical and Engineering Aspects

journal homepage: www.elsevier.com/locate/colsurfa

A novel approach for nanobubble generation toward biomedical applications

Lingxi Ouyang [a,b,1], Helena H.W.B. Hansen [a,b,1], Haotian Cha [a,b], Xueyu Ji [a,b], Jun Zhang [a,c], Qin Li [a,c], Beng Hau Tan [d], Quang Thang Trinh [a], Nam-Trung Nguyen [a,*], Hongjie An [a,b,**]

[a] Queensland Micro, and Nanotechnology Centre, Griffith University, 170 Kessel Road, Nathan, QLD 4111, Australia
[b] School of Environment Science, Griffith University, 170 Kessel Road, Nathan, QLD 4111, Australia
[c] School of Engineering and Built Environment, Griffith University, 170 Kessel Road, Nathan, QLD 4111, Australia
[d] Shenzhen Institute of Advanced Study, University of Electronic Science and Technology of China, Shenzhen 518110, China

GRAPHICAL ABSTRACT

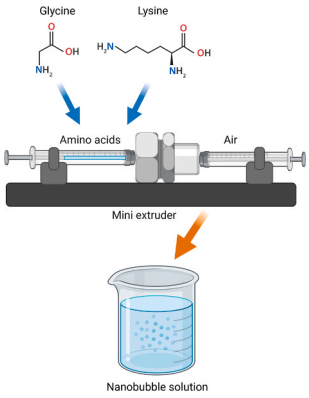

ARTICLE INFO

Keywords:
Nanobubbles
Amino acids
Mini-extruder
Stability
Ultrasound

ABSTRACT

The stability of free-standing nanobubbles is a long-standing controversial problem due to the Laplace pressure catastrophe at the nanoscale. In most industrial circumstances, a large quantity of surfactants is required as stabilisers or emulsifiers to generate stable bubbles or foams. However, when surfactants exceed a certain level, they can adversely affect living organisms and pose environmental risks. Towards biomedical use, we investigated nanobubble generation through a mini-extruder in amino acid solutions. Herein, we considered glycine (having two acid dissociation constants, i.e. pK_a values) and lysine (having three pK_a values) as two model amino acids, conducting experiments with various concentrations (0.1 M, 0.5 M and 1 M), along with different pH values (above, equal to, and below the isoelectric points of each amino acids; 5.97 for glycine and 9.74 for lysine). Our results showcased the proof of concept that amino acids can stabilise nanobubbles in bulk for a few days. We achieved remarkable products of nanobubbles via nanopores by extrusion, with reproducible size

* Corresponding author.
** Corresponding author at: Queensland Micro, and Nanotechnology Centre, Griffith University, 170 Kessel Road, Nathan, QLD 4111, Australia.
E-mail addresses: nam-trung.nguyen@griffith.edu.au (N.-T. Nguyen), hongjie.an@griffith.edu.au (H. An).
[1] Contributed equally.

https://doi.org/10.1016/j.colsurfa.2024.134773
Received 27 May 2024; Received in revised form 27 June 2024; Accepted 8 July 2024
Available online 8 July 2024

distribution and stability. We also compared the extrusion protocol with the commonly used ultrasound method. It turned out that extrusion generated samples with smaller sizes and higher concentrations than sonication. This study provides a reliable protocol for generating small-scale nanobubbles for biomedical use, showing great potential in drug delivery for medical treatment.

1. Introduction

Utilising micrometre-scale monodisperse gas bubbles as contrast agents in biological ultrasound imaging has been a well-established technique for decades [1]. However, the anticipated applications of these gas spheres, with sizes ranging from micrometres to hundreds of nanometres, extend far beyond this scope. Recent reports have demonstrated various nanobubble applications in enhancing the effectiveness of disease treatment at the cellular and molecular levels. Additionally, due to their biocompatibility combined with the ability to functionalise their surface to decrease detection in vivo, nanobubbles are considered suitable for various types of drug delivery, including controlled and targeted delivery [2]. Additionally, in some studies, nanobubbles have been suggested to possess anti-inflammatory, antibacterial, and wound healing-promoting effects [3]. However, despite the current advanced techniques for industry-scale preparation of nanobubble solutions, their biocompatibility is the greatest challenge in applying these products in biological fields [4]. In other words, nanobubbles intended for in vivo applications must ensure sterility and high stability, maintaining a consistent concentration and size over a certain period of time.

To date, the stability of bulk nanobubbles generated in pure water remains controversial [5–11]. Internal gas pressure will significantly increase to tens of bars when the bubble size reduces to 100 nm as a result of the Laplace pressure over the reduced curvature. Classic diffusion theory predicts that nanobubbles will shrink rapidly in water in a timescale of less than 1 ms [12]. However, experimentalists reported the existence of nanobubbles over a larger timescale [13–15]. Rather than attempting to produce bubbles in pure water, a more common approach is to stabilise them with surfactants [16–19]. However, the widespread use of surfactants such as sodium dodecyl sulphate or cetyltrimethylammonium bromide typically has the serious downside of biological toxicity. Although some reports have utilised phospholipids or polymers to enhance the stability of nanobubbles, complex macromolecules may lead to changes in bubble size [20], affecting the controllability of fabrication. Moreover, introducing lipids is non-trivial and may involve organic solvents. In addition, it may be necessary to introduce several other molecules may to meet biocompatibility requirements [21–23]. We hypothesise that non-toxic and biocompatible small molecule amino acids (such as glycine and lysine) may be a safer and more convenient approach to meet the biocompatibility requirements put forth for biological application of nanobubbles.

Amino acids are natural biological components that not only come together to synthesise proteins but are also found in neurotransmitters and hormones [24]. They vary in size and configuration, each having their own unique feature that determines its function within the generated compound. Amino acids, with the exception of glycine, can be found in both L and D conformations, with the former being used for protein synthesis in mammals, and the latter generally being found in bacterial cell walls. In addition, D amino acids are associated with energy breakdown, as well as diseases such as Alzheimer's, and are therefore considered toxic to humans [25]. Applying the L conformation of amino acids as a protective or targeting layer on nanobubbles lowers the risk of adverse effects as degradation of this layer in vivo simply releases low concentrations of non-toxic components. In addition, as amino acids function to bind to each other, the generation of customisable coatings is a possibility.

This study pursues a simple approach to produce low-toxic biocompatible nanobubbles for biomedical applications, addressing the challenge of creating stable nanobubbles with conventional technology. Traditional methods such as hydrodynamic cavitation, compression-decompression cycling, or probe sonication often require large and expensive equipment that is difficult to sterilise and poses a risk of contaminating cell cultures. To overcome these limitations, we are inspired by our previous work on lipid bilayers using a mini-extruder that is commonly used to generate monodispersed liposomes at the nanoscale [26,27]. The mini-extruder is cheap, easy to handle at various temperatures, and can be sterilised in an autoclave, making it ideal for small-scale production in a lab. The 200 nm nanopore membrane incorporated in the mini-extruder system of our work renders a credible size control of nanobubbles and, meanwhile, filters out the bacteria, preventing contaminations. In addition, this method allows for easy fusion of various gases for different purposes. The integration facilitates the research of nanobubbles in biomedical engineering for drug delivery, ultrasound imaging, and cancer therapy.

In this study, we utilise common amino acids to generate bulk nanobubbles with a mini-extruder in conjunction with nanopore membranes. Herein, we chose glycine (with two pK_a values: pK_1 = 2.34, pK_2 = 9.60, and pI of 5.97) and lysine (with three pK_a values: pK_1 = 2.18, pK_2 = 8.95, pK_3 = 10.53, and pI of 9.74) as two model amino acids [28]. Amino acids have a key property that they are positively charged at a pH below pK_1 and negatively charged above the pK_2 or pK_3, and exist on average as neutral zwitterionic molecules at the isoelectric point (IEP or PI). This characteristic enables amino acids to interact with gas bubbles differently depending on the pH. Thus, we hypothesise that nanobubbles can be stabilised with surface charges under varying pH conditions. In our experiment, the mini-extruder, commonly used to prepare monodisperse vesicles and liposomes, is utilised to generate nanobubbles in amino acid solutions after being equipped with a submicron porous membrane. We characterised and compared the bubble size, concentration, and solution zeta potential of the nanobubble solutions obtained at different concentrations and pH levels of amino acids and compared them with the corresponding control group.

2. Materials and methods

2.1. Materials

Glycine (≥ wt 99 %) and L-lysine (≥ wt 99 %) were directly purchased from the Sigma-Aldrich. Milli-Q water was from the Milli-Q® Direct Water Purification System with a conductivity of 18.2 MΩ. The stock solution for amino acids was prepared with a concentration of 1 M. Hydrochloric acid (HCl, 37 % w/w) was purchased from Sigma-Aldrich, and sodium hydroxide (NaOH, ≥ 99 wt%) was purchased from ChemSupply for solution pH adjustment.

2.2. Nanobubble solution generation

The stock solutions of the amino acids were made with Milli-Q water (measured pH = 7 ± 0.1) at a concentration of 1 M. For the stock solution and the corresponding diluted solutions, the pH measured by pH metre (HI5521, HANNA) is 6.2 ± 0.01 in glycine and 10.3 ± 0.01 in lysine. Based on the glycine's IEP of 5.97 and that of lysine is 9.74, we prepared three different pH samples (above, near, and below the IEP of the amino acid) solutions for glycine at pH = 1.9 (< IEP), pH = 5.9 (~ IEP), and pH = 10.0 (> IEP), and another three for lysine at pH = 1.9 (< IEP), pH = 9.8 (~ IEP), and pH = 11.4 (> IEP), to verify the pH effect on the nanobubble's size and concentration. The pH of the samples was adjusted by sodium hydroxide solution (1 M) and the hydrochloric acid

solutions (10 % w/w).

The mini-extruder (Avanti Polar Lipid, Inc.) was used to generate nanobubbles. We first prepared a 200 nm polycarbonate membrane filter (Isopore™) and placed it into the centre of the mini-extruder between the two syringe tips (inset, Fig. 1). We then filled three-quarters of one syringe (Fig. 1, left) with the desired amino acid solution and one-quarter of the other syringe (Fig. 1, right) with air. Subsequently, we assembled both syringes onto the mini-extruder, pushing the solution in the left syringe slowly through the membrane to the syringe on the right, followed by the reverse operation of pushing solution/air in the right syringe through the filter to the syringe on the left. The liquid was cycled between the two syringes 10 times. Finally, the solution is collected from the syringe on the right for characterisation.

A Probe sonicator (VCX 750, Sonics & Materials, Inc.) was used to generate nanobubble solutions for comparison. The amplitude was set to 100 %, and a 5-second pulse wasapplied when sonicating. The amino acid solutions were sonicated for 10 minutes in total, and an ice bath was applied to maintain the temperature of the samples.

2.3. Characterisation

The generated nanobubble solutions and the control group samples (stock solutions with no nanobubbles) were characterised by a Nanoparticle Tracking Analysis (NTA) system (Nanosight NS300, Malvern Panalytical) and Dynamic Light Scattering (DLS) instrument (LiteSizer 500, Anton Paar). The zeta potential was measured with LiteSizer 500.

3. Results and discussion

We hypothesise that: (i) nanobubbles can be generated when gases infuse in water by passing through nanopores; (ii) amino acids can act as biological surfactants to stabilise nanobubbles. In this study, we tried to verify our hypothesis and generate nanobubble in amino acid solutions through nanopores via a mini-extruder. We examined the size distribution and zeta potential of nanobubbles at different pH levels. Additionally, we compared the efficacy of nanobubble generation between the mini-extruder and sonication methods.

The mini-extruder is commonly employed for the preparation of monodisperse vesicles, liposomes, and lipid bilayers [27,29,30]. As illustrated in Fig. 1, a porous polycarbonate membrane filter is placed between two Teflon O-rings and positioned within the sealed chamber of the extruder, with needles of glass syringes attached to both sides in an air-tight manner. As pressure increases inside the extruder during the advancement of one piston toward the other, gas oversaturation occurs, leading to cavitation and bubble formation as the solution passes through the porous membrane. Utilising a substantial amount of lipids and surfactants, nanobubble production using the mini-extruder has been demonstrated to be feasible [31]. Therefore, we attempted to prepare nanobubble solutions solely using simple amino acid solutions via the mini-extruder and validated their feasibility through various characterisation techniques.

3.1. Nanobubbles by extrusion

The solutions produced by the mini-extruder were analysed using NTA to obtain the concentration of nanobubbles. Fig. 2 shows that both glycine (pH = 6.2) and lysine (pH= 10.3) solutions demonstrated a large concentration of nanoparticles after ten extrusion cycles at the three concentrations (0.1 M, 0.5 M, and 1 M), with sizes ranging from approximately 70 to 150 nm. The results show that the nanobubble size shifts towards larger values as the concentration increases for both glycine and lysine solutions. Meanwhile, at the lowest amino acid concentration of 0.1 M (black curve), the nanobubble size distribution exhibited excellent uniformity, with the half-width being smaller than other concentrations within the same group. This is particularly evident in the lysine solution, where the peak intensity reached nearly 8×10^6 particles/ml. However, compared to the lysine solution, the peak of the nanobubble size distribution in the glycine solution was lower, approaching 4×10^6 particles/ml. Nevertheless, the peak intensity in lysine solution at all three concentrations exceeded 5×10^6 particles/ml.

The concentration data (Fig. 2c and d), clearly indicates that the total concentration of nanobubbles in the lysine solution is higher than that in the glycine solution. In the glycine solution, the concentration of nanobubbles is similar for both 0.1 M and 0.5 M, at approximately 1.5×10^8 particles/ml. In contrast, the concentration in the 1 M solution is significantly higher, reaching 2.6×10^8 particles/ml. In lysine solution,

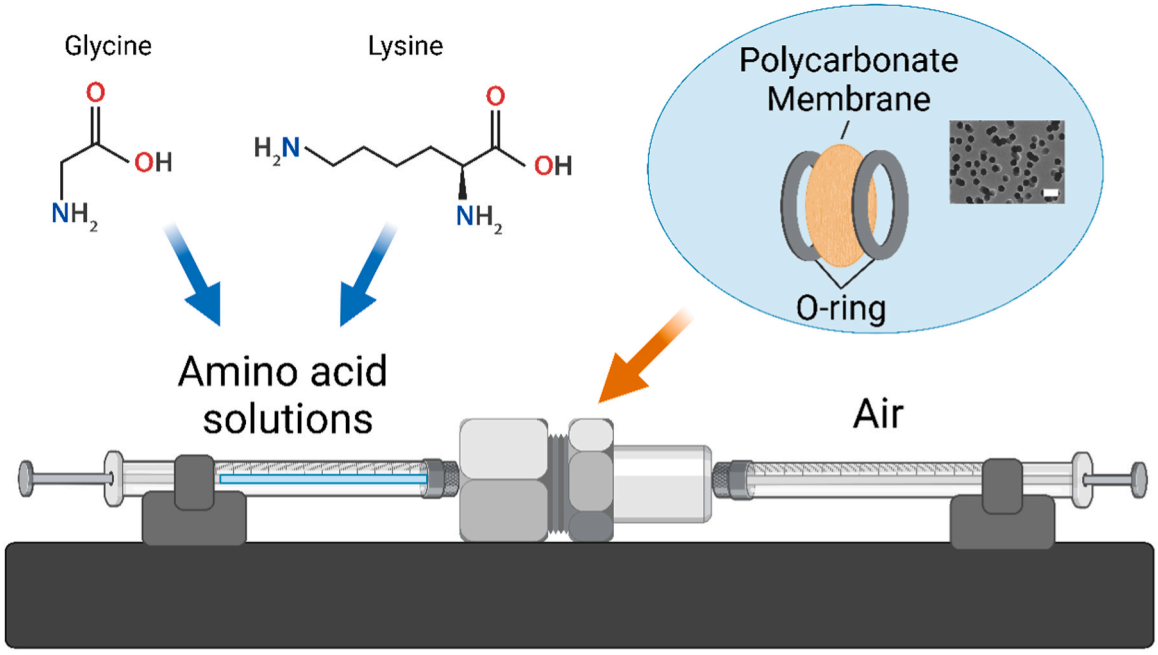

Fig. 1. Schematic description of the generation of amino acid nanobubble solutions generation using a mini-extruder. The inset shows the internal setup of the mini-extruder, and the SEM image illustrates the pores on the polycarbonate membrane with a scale bar of 500 nm. Made with Biorender.com.

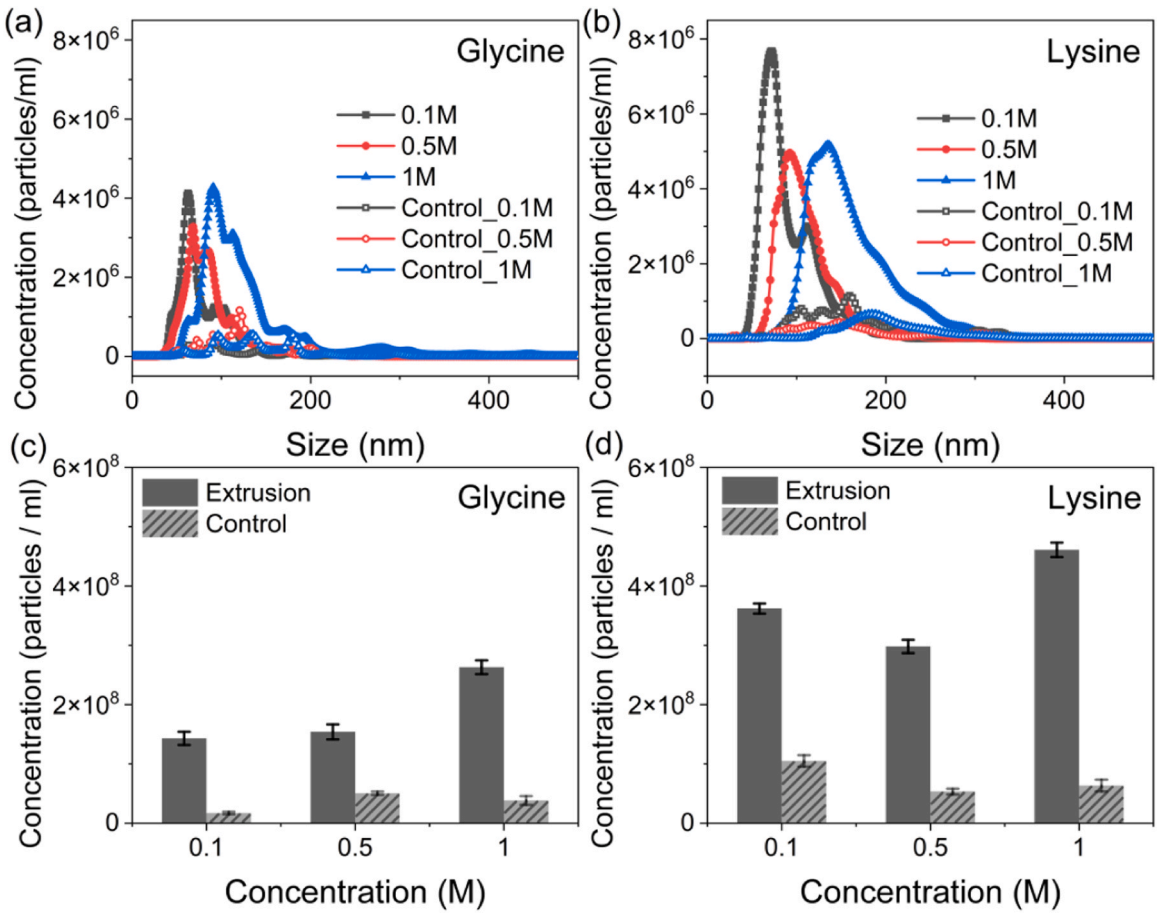

Fig. 2. Concentration of nanobubbles (from NTA) generated by the extruder in 0.1 M, 0.5 M, and 1 M (a) Glycine and (b) Lysine solution (solid) and the control group results (hollow). The control group shows negligible amounts of bubbles. The total concentration of nanobubbles generated by the extruder in 0.1 M, 0.5 M, and 1 M (c) Glycine and (d) Lysine solution and the control group. The pH of glycine groups has a pH of 6.2, and the lysine groups have a pH of 10.3.

the concentration of nanobubbles in lysine solution exhibits a distinctly different phenomenon. Although the concentration of nanobubbles in the 1 M solution (4.6×10^8 particles/ml) remains higher than other concentrations, the nanobubble concentration in the 0.5 M solution (3.0×10^8 particles/ml) is less than that in the 0.1 M solution (3.6×10^8 particles/ml), corresponding to the outstanding size distribution of the 0.1 M lysine solution shown in Fig. 2. It is interesting that sizes of nanobubbles increase with the concentration of amino acids (Fig. 2), independent of the type of amino acids. In glycine solution, the average size of nanobubbles increases from approximately 82.1 ± 1.7 nm (0.1 M glycine) to approximately 122.4 ± 1.5 nm (1 M glycine). In lysine solution, the average size of nanobubbles increases from 91.6 ± 1.1 nm (0.1 M lysine) to 160.8 ± 0.8 nm (1 M lysine).

Compared to glycine, the average size of nanobubbles in lysine samples is larger, consistent with the findings of Nafi et al. regarding the inhibition of bubble coalescence in amino acid solutions [32]. The team investigated the transmittance of bubble solutions in different amino acid solutions using a bubble column evaporator method and found that the free state of amino acids is highly efficient in preventing bubble aggregation and generating smaller bubbles. Due to its smaller size and weak hydrophilic properties, glycine, even in high-concentration solutions, forms aggregations around the bubbles, but the thickness of these aggregation layers is smaller than that of long-chain lysine. With its long carbon chain, aggregates in high-concentration lysine nanobubble solutions can be quite large, potentially protruding into the solution and causing some steric hindrance [33], making the aggregates appear longer. In the case of bubbles, they are predominantly located on the bubble surface, with side chains extending out, similar to their behaviour in proteins [34,35].

Spontaneous aggregation of amino acids may occur due to the presence of hydrogen bonds. However, without bubbles or other homogeneous media, there is no effective way to control the size of amino acid spontaneous aggregation, leading to a broad size distribution observed in the NTA results. In systems containing bubbles, bubbles may mediate the behaviour of amino acids. Our previous paper found nanobubbles can effectively remove proteins from surfaces and prohibit proteins from attaching to surfaces under water [36], indicating a strong interaction between proteins and nanobubbles. Amino acid molecules are basic components of proteins, but smaller in size so that they can perform similarly to proteins. Interactions between bubbles and amino acids can prevent them from randomly aggregating. Comparing the data of the two groups of amino acids, we can conclude that lysine exhibits better concentration and more uniform size distribution.

3.2. *Lifespan of nanobubbles*

To evaluate the lifetime of nanobubbles, we continuously monitored the size of generated nanobubbles using a DLS instrument for 72 hours (Fig. 3). During these three days, the nanobubble solution generated by the mini-extruder was kept in the same cuvette in the DLS instrument and measured at a set temperature 25℃. Fig. 3 clearly shows uniform size at initial and dynamic size changes during the lifespan. The DLS mode size of nanobubbles in the glycine solution is smaller than that in the lysine solution, which is consistent with NTA results. Fig. 3a shows the size of nanobubbles in glycine solutions gradually increases, indicating the dynamic changes of bubbles, suggesting the Ostwald ripening

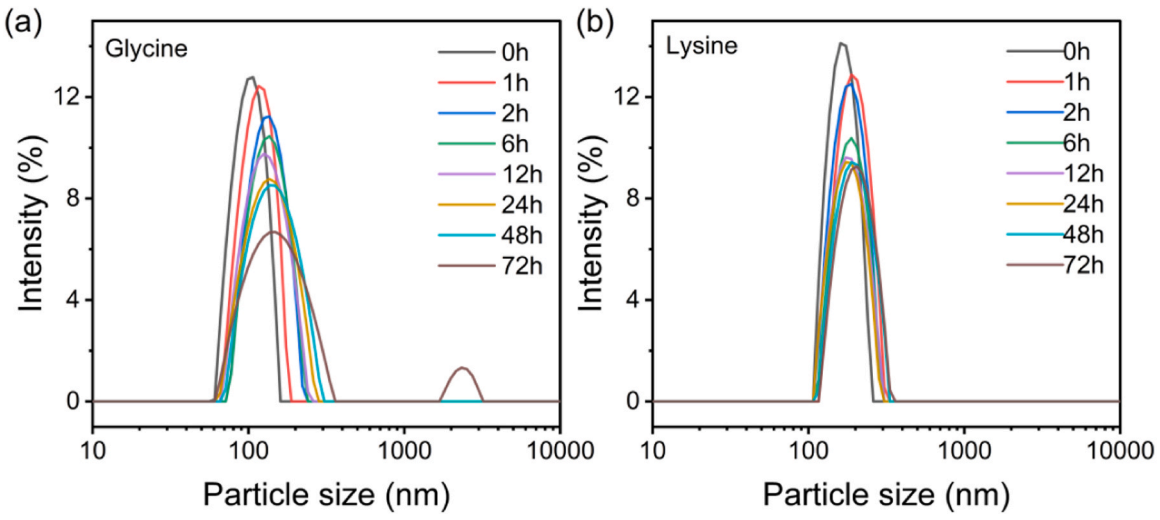

Fig. 3. Stability of nanobubble Dynamic light scattering spectra of the particle sizes, tracked over 72 hours when the nanobubbles are generated by the extruder in 0.1 M (a) Glycine at pH 6.2 and (b) Lysine solution at pH 10.3.

of the nanobubbles. An outlier at 72-hour in Fig. 3a indicates the emergence of some large-size domains, which could be bubble growing due to the coalescence of nanobubbles along with the Ostwald ripening over time. Fig. 3b shows that the lysine-nanobubble particles are relatively stable in a lifespan of 72 hours, but intensity gradually reduced, suggesting good stability of the lysine nanobubble solution. The dynamic changes in size also render the colloids under characterisation as gas nanobubbles that are subject to diffusion by molecules other than nanoparticles or nanodroplets.

We measured the zeta potential distribution of nanobubble solutions at different concentrations of amino acids, as shown in Fig. 4. It is interesting that, regardless of whether it was glycine or lysine, the nanobubble solutions exhibited zeta potential values above but close to 0 mV. In the 0.1 M, 0.5 M, and 1 M glycine nanobubble solutions, the zeta potential values were 1.9 mV, 2.1 mV, and 2.7 mV, respectively. The lysine solutions were 1.1 mV, 0.8 mV, and 1.6 mV, respectively. The two sets of data did not show significant differences, suggesting bubble-induced changes in the groups present in the two amino acids. It is uncertain whether the interface of gas/water affects the charges linked to the dissociation of amino acids, which are specific to pH.

3.3. pH study

Amino acid molecules have both -NH_2 (basic functional) and -COOH (acidic functional) groups that present in different forms at different pH. Since these groups have different acid dissociation abilities, so it is possible, via manipulation of the pH, to generate an amino acid that carries no net charge; i.e. they are in zwitterion form at their IEP. In solutions where pH determines the ions as H^+ or OH^-, amino acids exhibit different behaviours based on the pH relative to their isoelectric point. When the pH is higher than the isoelectric point, the acidic functional groups of the amino acids are fully neutralised, resulting in a net negative charge. Conversely, when the pH is lower than the isoelectric point, the basic functional groups are no longer dissociated, causing the amino acids to carry a net positive charge. Here, we chose the samples with a concentration of 0.1 M for both amino acid solutions to observe the effect of pH on the nanobubble generation[37,38]. In glycine, we chose three different pH samples of 1.9 (<IEP), 5.9 (= IEP) and 10.0 >IEP; in lysine, we chose another three different pH samples of 1.9 (<IEP), 9.8 (= IEP) and 11.4 >IEP.

Fig. 5 shows the concentration and size distribution of nanobubbles generated in glycine and lysine solutions under varying pH. At pH > IEP,

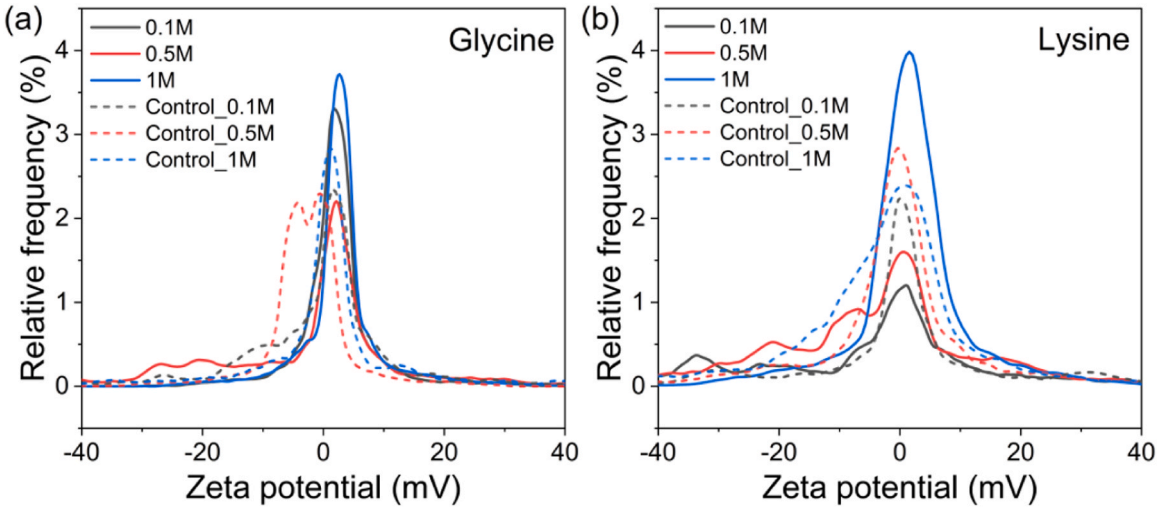

Fig. 4. Zeta potential distribution of nanobubbles generated by the extruder in 0.1 M, 0.5 M, and 1 M (a) Glycine and (b) Lysine solution and the control group results. The pH of glycine groups has a pH of 6.2, and the lysine groups have a pH of 10.3.

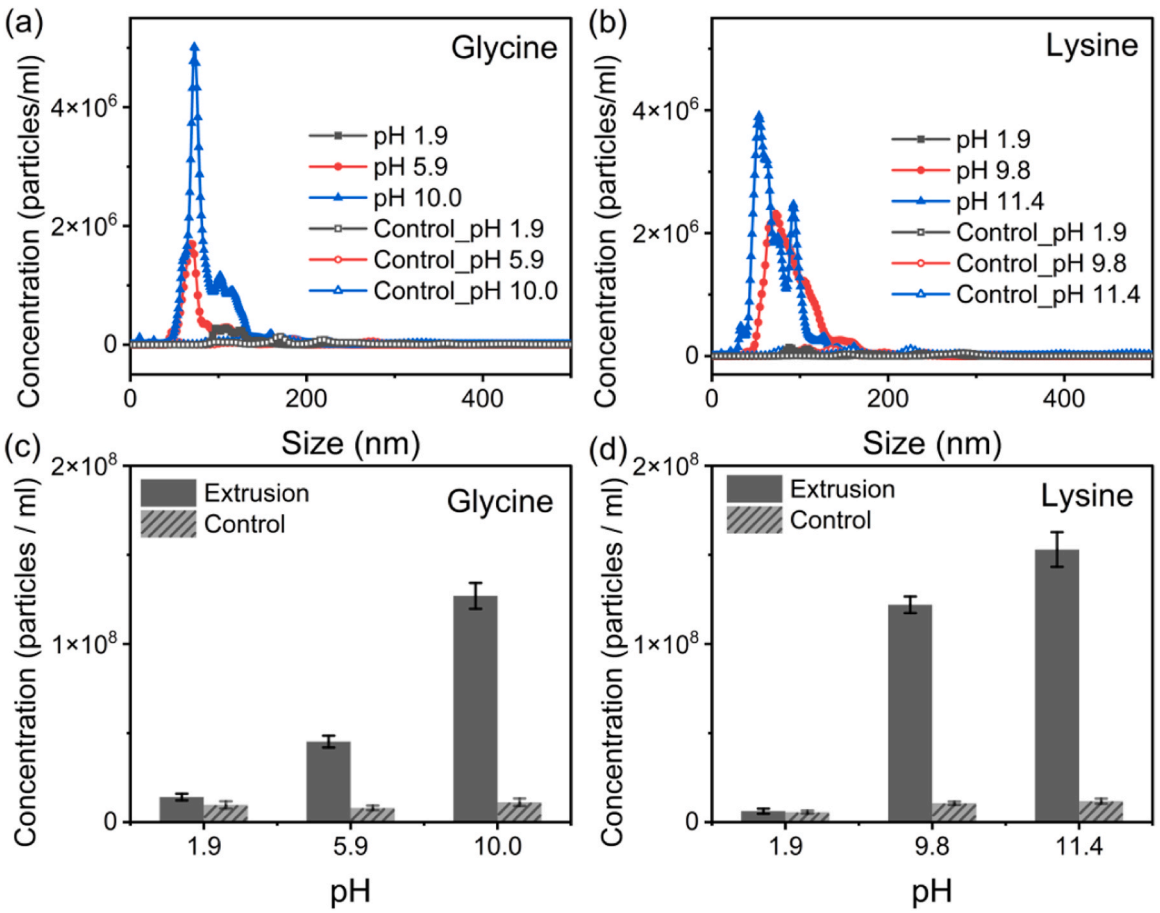

Fig. 5. NTA concentrations of nanobubbles at different pH generated by the extruder in (a) 0.1 M Glycine with pH 1.9, pH 5.9, and pH 10.0 and (b) 0.1 M Lysine solution with pH 1.9, pH 9.8, and pH 11.4. Effect of pH on total nanobubbles concentration of nanobubbles generated by the extruder in (c) 0.1 M Glycine with pH 1.9, pH 5.9, and pH 10.0 and (d) 0.1 M Lysine solution with pH 1.9, pH 9.8, and pH 11.4.

both cases of glycine and lysine exhibit high concentrations. Nanobubbles in glycine solutions (Fig. 5a) have a large concentration peak of ~5 × 10^6 particles/ml at a size of ~73 nm at pH 10.0. Nanobubbles in lysine solutions have a concentration peak of ~4 × 10^6 particles/ml at a size of ~54 nm at pH 11.4 (Fig. 5b). At IEP, the glycine nanobubbles have a concentration peak of ~1.8×10^6 particles/ml at a size of ~71 nm, and lysine nanobubbles have a concentration peak of ~2.3×10^6 particles/ml at a size of 74 ± 2 nm. However, at pH < IEP (pH 1.9), both cases show negligible peak concentration of the nanobubble solution < 5×10^5 particles/ml. It is a significant decrease at pH 5.9 compared to pH 6.2. In the case of lysine (Fig. 5b), the particle concentrations at pH 9.8 and pH 11.4 are also lower than those at pH 10.3

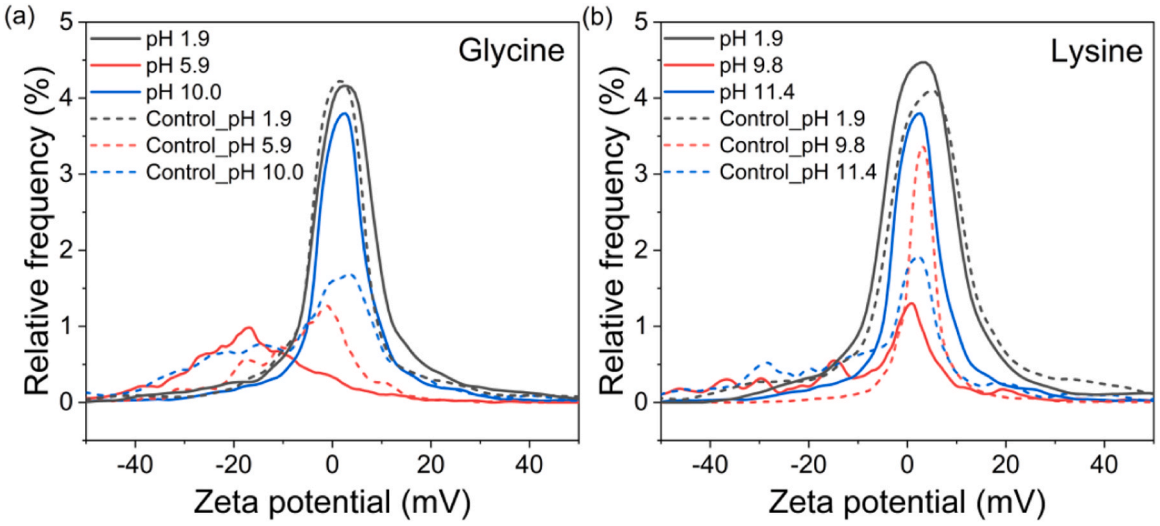

Fig. 6. Zeta potential distribution of nanobubbles generated by the extruder in (a) 0.1 M Glycine with pH 1.9, pH 5.9, and pH 10.0 and (b) 0.1 M Lysine solution with pH 1.9, pH 9.8, and pH 11.4.

(Fig. 2b).

For the mean size of the nanobubbles in each group, we do not consider the size at acidic conditions (pH 1.9), as their concentrations are negligible. Near the IEP, their sizes are 80 ± 4 nm (glycine) and 93 ± 2 nm (lysine). In basic environments (pH > IEP), the lysine nanobubble's average size decreases to around 72 ± 2 nm while the size of the glycine nanobubble grows a little to 87 ± 2 nm. The average sizes near IEP are comparable to the sizes of nanobubbles in unadjusted pH 0.1 M amino acid solutions, suggesting that when the pH is close to IEP, changes in pH do not significantly affect nanobubble size. However, for lysine nanobubbles, the basic solution leads to a considerable shrinking of the bubble's size around 20 nm, implying an impact of negative charge on lysine nanobubbles.

Fig. 6 illustrates the zeta potential of nanobubble solutions of different amino acids at various pH values. We observe that under varying pH values, except for the glycine nanobubble solution at the IEP, almost all groups exhibit a positive zeta potential, above and close to 0 mV. The glycine solution at IEP shows a zeta potential of −20 mV. At the IEP, there are no net ions on glycine molecules, and glycine molecules are small, and their binding to nanobubbles may not add any zeta potential to bubbles. The measured zeta potential is close to that of uncoated nanobubbles of −20 mV as previously reported [39]. This may explain the large shift in zeta potential in Fig. 6a for glycine and Fig. 6b with lysine samples at the IEP.

At pH 1.9, we deem there are no nanobubbles as their concentration is negligible (Fig. 5a and b). The pH of 1.9 is lower than the IEP of both bubbles (pH 2 ∼ 3) and amino acids; thus, the two are positively charged. Such a low pH value can significantly change the Stern layer structures and reduce the thickness of the electrical double layer, resulting in a strong positive charge density at the gas-water interface. Once nanobubbles were formed, the outward electrostatic pressure could be large enough to tear them apart as the inward Laplace pressure cannot counteract it [9,11]. Consequently, nanobubbles rupture, which is reflected in Fig. 5., where both glycine and lysine solutions exhibit negligible total concentrations at pH 1.9.

At the IEP of amino acids, they (pH 5.9 for glycine) exist as zwitterion molecules, carrying no net charge. This will add marginal surface charges to nanobubbles, and the measured zeta potential of nanobubbles could be nanobubble themselves with a glycine skin. Similarly, at pH 9.8, lysine molecules are at their IEP. Unlike glycine, lysine molecules have a longer side chain, and their interactions are slightly stronger than those of glycine, leading to slightly larger nanobubble sizes. The formed encapsulating lysine layer around nanobubbles will also interfere with zeta potential.

At pH > IEP of amino acids, both amino acids carry a net negative charge (glycine at pH 10.0 and lysine at pH 11.4). This negative charge stabilises nanobubbles with electric repulsion between them. The repulsion leads to nanobubbles remaining small and numerous, akin to the behaviour of glycine. However, in some studies, nanobubbles' long lifespan is associated with hydrogen bonds forming at the gas-liquid interface with the aqueous solution, forming a barrier that reduces gas diffusion[40]. The side chain of lysine sometimes participates in forming hydrogen bonds with negatively charged non-protein atoms[41,42]. The naturally occurring hydrogen bonds between nanobubbles and the water environment might add an extra layer of stability to the nanobubble-amino acid particles. This stability layer takes over the hydrogen bonds generated by the nanobubbles, allowing the amino acids to interact with the nanobubbles and partially encapsulates the hydrophobic chains around the nanobubbles. Therefore, at pH values higher than the IEP, lysine solutions exhibit larger nanobubble sizes and higher particle concentrations compared to glycine solutions.

In comparing the sizes of nanobubble-amino acid particles, it is observed that the average sizes of the particles under different protonation states are very similar, with lysine-containing particles being only about 25 nm larger in each case. Glycine is the smallest and simplest amino acid, while lysine is one of the longest, so it seems counterintuitive that they should result in similarly sized particles. However, lysine possesses a long hydrophobic chain, which likely interacts with and wraps around the hydrophobic nanobubbles. In this way, the interaction of the amino acid does not result in hair-like particles. Similar to glycine, the backbone is the only part of lysine that interacts with the aqueous solution, leading to particles with a similar appearance. This interaction mechanism, combined with the filter in the extruder, defines the size of the generated bubbles, resulting in particles of similar sizes. The only difference lies in the packing of the amino acids and the presence of the additional amine group in lysine. Given that the concentrations of negatively charged amino acids are relatively similar (see Fig. 5c and d), and knowing that the amino acid concentration is the same for all samples, it can be inferred that if the hydrophobic side chain of lysine wraps around the bubble, there might be additional unbound lysine in the solution. Alternatively, the side chain might enter the bubble to avoid the aqueous environment, leaving the backbone on the surface. This configuration would result in lysine's outward structure being similar to glycine's but smaller in size.

3.4. Comparison of extrusion and sonication

To further explore the characteristics of nanobubble solutions generated by the extruder, we processed 0.1 M amino acid solutions using extruder and probe ultrasound methods, yielding different outcomes. As depicted in Fig. 7a, probe sonication produces a broader size distribution and lower concentration than the extrusion protocol. The nanobubble size distribution induced by probe sonication appears broader, ranging from approximately 50 nm to 200 nm, with multiple size distribution peaks evident in the lysine solution. In contrast, the nanobubble size distribution generated by the extruder exhibits higher peak intensities and better uniformity in size distribution. Fig. 7b illustrates that the average size of nanobubbles produced by the extruder is smaller than those produced by probe sonication. Furthermore, in Fig. 7c, the total concentration of nanobubble solutions generated by the mini-extruder in lysine solutions demonstrates superior results compared to the other three groups. Fig. 7d shows the zeta potentials of the four samples. The two samples treated with probe sonication have a negative zeta potential of ∼ −30 mV.

This greater uniformity observed by the extruder system is attributed to the use of a filter, which was not applicable to the probe sonicator. However, we note that the two methods result in relatively similar-sized particles, with the sonicator samples only being ∼40 nm larger. This indicates the readiness of the free amino acids to bind to the generated nanobubbles, as well as the preference of amino acids for bubble size, without the need for mechanical sheer to drive the interactions. The major difference is observed in the particle's zeta potential (Fig. 7d). The particles produced by probe sonication have a much lower zeta potential, −30 mV, which is comparable to the zeta potential of naked nanobubbles [43,44]. The extruder particles exhibit positive zeta potential but close to 0 mV in this study (Figs. 4 and 6), indicating different stability mechanisms from ultrasound.

Ultrasonic mechanical waves have been applied in the modification of proteins, which led to the unfolding of proteins, and the side chains of amino acids were altered or enhanced hydrogen bond [45]. The change in the amino acid would then affect the interaction and subsequent orientation of the amino acid on/in the generated nanobubbles. During ultrasound treatment, cavitation occurs and generates free radicals that facilitate hydrogen bonding between water molecules and/or amino acids. Gathering -OH at the interface of the gas bubble and water possibly induces a negative zeta potential, which further stabilises the bubbles.

4. Conclusion

In summary, this paper presents the generation of nanobubbles stabilised by amino acids using a mini-extruder. We successfully generated

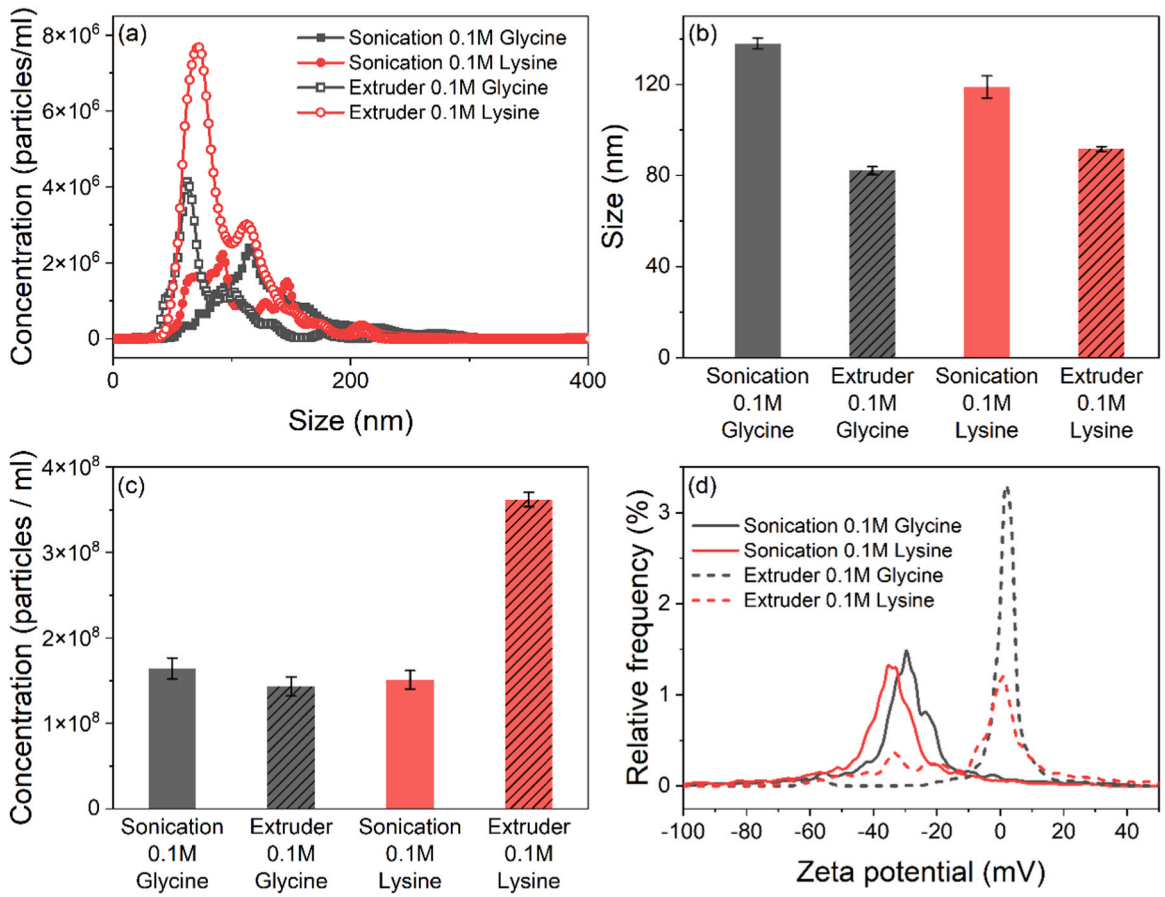

Fig. 7. (a) Size distribution, (b) average size, (c) total nanobubbles concentration, and (d) zeta potential distribution results in 0.1 M glycine (pH 6.2) and lysine (pH 10.3) nanobubble solutions. The data of (a), (b), and (c) were collected using a nanoparticle tracking analysis (NTA) system. The (d) data was collected using a dynamic light scattering (DLS) system.

stable, monodispersed nanobubbles of a high concentration that can persist for a few days in amino acid solutions. When comparing the glycine and lysine solutions, the latter produced a higher nanobubble concentration. Increasing the amino acid concentration leads to larger sizes and more bubbles. Again, lysine gave rise to higher concentrations and larger sizes than glycine. We achieved an acceptable concentration of nanobubbles (~ 100 nm) using a small number of amino acids (~ 0.1 M). Our pH study shows that nanobubbles are not favourable at low pH ~ 2. At a pH close to the IEP of amino acids, where they are predominantly found in their zwitterionic configuration, glycine contributes minimally to the size and concentration of nanobubbles as manifested by negative zeta potential, while lysine has slightly larger nanobubbles due to its longer side chain. We achieved a substantial amount of nanobubbles at a pH above the IEP of amino acids as the negative charge stabilises nanobubbles through electrostatic repulsion.

When comparing sonication and extrusion, we found that extrusion produced a sample with a narrower size distribution and higher concentration in both glycine and lysine solutions. The biggest difference between extrusion and sonication was the resulting zeta potential. Sonication produced negatively charged bubbles, while extrusion produced slightly positive charges. This study provides evidence of generating nanobubbles coated with amino acids. It is a relatively simple process that allows small-scale production of nanobubbles, offering an opportunity for future drug delivery using nanobubbles as carriers stabilised by amino acids.

CRediT authorship contribution statement

Nam-Trung Nguyen: Writing – review & editing, Supervision, Resources. **Qin Li:** Writing – review & editing. **Jun Zhang:** Writing – review & editing. **Quang Thang Trinh:** Writing – review & editing. **Beng Hau Tan:** Writing – review & editing. **Helena H.W.B. Hansen:** Writing – review & editing, Writing – original draft, Investigation. **Lingxi Ouyang:** Writing – original draft, Visualization, Methodology, Investigation, Formal analysis, Data curation. **Xueyu Ji:** Writing – review & editing. **Haotian Cha:** Writing – review & editing. **Hongjie An:** Writing – review & editing, Writing – original draft, Validation, Supervision, Resources, Project administration, Conceptualization.

Declaration of Competing Interest

The authors declare that they have no known competing financial interests or personal relationships that could have appeared to influence the work reported in this paper.

Data Availability

Data will be made available on request.

Acknowledgments

H.A. gratefully acknowledges the funding support of the Australian Research Council through the ARC Future Fellowship (FT180100361) and ARC Discovery Project (DP230100556) Q.T.T. and N.-T.N. would like to acknowledge the support from the Australian Research Council for the ARC Laureate Fellowship (FL230100023). B.H.T acknowledges the support of the National Natural Science Foundation of China Program for Excellent Young Scientists (overseas).

References

[1] P. Frinking, T. Segers, Y. Luan, F. Tranquart, Three decades of ultrasound contrast agents: a review of the past, present and future improvements, J. Med. Ultrasound 46 (2020) 892–908.

[2] H.H.W.B. Hansen, H. Cha, L. Ouyang, J. Zhang, B. Jin, H. Stratton, N.-T. Nguyen, H. An, Nanobubble technologies: applications in therapy from molecular to cellular level, Biotechnol. Adv. 63 (2023) 108091.

[3] A.W. Foudas, R.I. Kosheleva, E.P. Favvas, M. Kostoglou, A.C. Mitropoulos, G. Z. Kyzas, Fundamentals and applications of nanobubbles: a review, Chem. Eng. Res. Des. 189 (2023) 64–86.

[4] A.A. Paknahad, L. Kerr, D.A. Wong, M.C. Kolios, S.S.H. Tsai, Biomedical nanobubbles and opportunities for microfluidics, RSC Adv. 11 (2021) 32750–32774.

[5] M. Alheshibri, V.S.J. Craig, Armoured nanobubbles; ultrasound contrast agents under pressure, J. Colloid Interface Sci. 537 (2019) 123–131.

[6] D. Rak, M. Ovadová, M. Sedlák, (Non)existence of bulk nanobubbles: the role of ultrasonic cavitation and organic solutes in water, J. Phys. Chem. Lett. 10 (2019) 4215–4221.

[7] N. Nirmalkar, A.W. Pacek, M. Barigou, On the existence and stability of bulk nanobubbles, Langmuir 34 (2018) 10964–10973.

[8] L. Ouyang, Q. Zeng, N.-T. Nguyen, B.H. Tan, H. An, Destabilizing surface bubbles with excessive bulk oversaturation, Colloids Surf. A 689 (2024) 133665.

[9] B.H. Tan, H. An, C.-D. Ohl, Stability of surface and bulk nanobubbles, Curr. Opin. Colloid Interface Sci. 53 (2021) 101428.

[10] B.H. Tan, H. An, C.-D. Ohl, Identifying surface-attached nanobubbles, Curr. Opin. Colloid Interface Sci. 53 (2021) 101429.

[11] B.H. Tan, H. An, C.-D. Ohl, How bulk nanobubbles might survive, Phys. Rev. Lett. 124 (2020) 134503.

[12] P.S. Epstein, M.S. Plesset, On the stability of gas bubbles in liquid-gas solutions, J. Chem. Phys. 18 (1950) 1505–1509.

[13] H. An, B.H. Tan, Q. Zeng, C.-D. Ohl, Stability of nanobubbles formed at the interface between cold water and hot highly oriented pyrolytic graphite, Langmuir 32 (2016) 11212–11220.

[14] N. Nirmalkar, A.W. Pacek, M. Barigou, Bulk nanobubbles from acoustically cavitated aqueous organic solvent mixtures, Langmuir 35 (2019) 2188–2195.

[15] H. An, G. Liu, R. Atkin, V.S.J. Craig, Surface nanobubbles in nonaqueous media: looking for nanobubbles in DMSO, formamide, propylene carbonate, ethylammonium nitrate, and propylammonium nitrate, ACS Nano 9 (2015) 7596–7607.

[16] X. Ma, M. Li, X. Xu, C. Sun, Coupling effects of ionic surfactants and electrolytes on the stability of bulk nanobubbles, Nanomaterials 12 (2022) 3450.

[17] E.D. Michailidi, G. Bomis, A. Varoutoglou, G.Z. Kyzas, G. Mitrikas, A. C. Mitropoulos, E.K. Efthimiadou, E.P. Favvas, Bulk nanobubbles: production and investigation of their formation/stability mechanism, J. Colloid Interface Sci. 564 (2020) 371–380.

[18] K. Ferrara, R. Pollard, M. Borden, Ultrasound microbubble contrast agents: fundamentals and application to gene and drug delivery, Annu. Rev. Biomed. Eng. 9 (2007) 415–447.

[19] J. Xu, A. Salari, Y. Wang, X. He, L. Kerr, A. Darbandi, A.C. de Leon, A.A. Exner, M. C. Kolios, D. Yuen, S.S.H. Tsai, Microfluidic generation of monodisperse nanobubbles by selective gas dissolution, Small 17 (2021) 2100345.

[20] M.S. Khan, J. Hwang, K. Lee, Y. Choi, J. Jang, Y. Kwon, J.W. Hong, J. Choi, Surface composition and preparation method for oxygen nanobubbles for drug delivery and ultrasound imaging applications, Nanomaterials 9 (2019) 48.

[21] L. Song, G. Wang, X. Hou, S. Kala, Z. Qiu, K.F. Wong, F. Cao, L. Sun, Biogenic nanobubbles for effective oxygen delivery and enhanced photodynamic therapy of cancer, Acta Biomater. 108 (2020) 313–325.

[22] X. Zhou, L. Guo, D. Shi, S. Duan, J. Li, Biocompatible chitosan nanobubbles for ultrasound-mediated targeted delivery of doxorubicin, Nanoscale Res. Lett. 14 (2019) 24.

[23] A.U. Sabancı, P. Erkan Alkan, C. Mujde, H.U. Polat, C. Ornek Erguzeloglu, A. Bisgin, C. Ozakin, S.G. Temel, Nanobubble ozone stored in hyaluronic acid decorated liposomes: antibacterial, anti-SARS-CoV-2 effect and biocompatibility tests, Int. J. Nanomed. 17 (2022) 351–379.

[24] M.J. Lopez, S.S. Mohiuddin, Biochemistry, essential amino acids, StatPearls Publishing, 2024.

[25] M. Abdulbagi, L. Wang, O. Siddig, B. Di, B. Li, D-amino acids and D-amino acid-containing peptides: potential disease biomarkers and therapeutic targets? Biomolecules 11 (2021) 1716.

[26] H.H.W.B. Hansen, G. Kijanka, L. Ouyang, N.-T. Nguyen, H. An, Surfactant-free oil-in-water nanoemulsions with nanopore membrane and ultrasound, J. Mol. Liq. 399 (2024) 124323.

[27] H. An, M.R. Nussio, M.G. Huson, N.H. Voelcker, J.G. Shapter, Material properties of lipid microdomains: force-volume imaging study of the effect of cholesterol on lipid microdomain rigidity, Biophys. J. 99 (2010) 834–844.

[28] F. Carey, R. Giuliano. Organic Chemistry, Fourth ed., McGraw-Hill Higher Education, 2013.

[29] C.-M.J. Hu, L. Zhang, S. Aryal, C. Cheung, R.H. Fang, L. Zhang, Erythrocyte membrane-camouflaged polymeric nanoparticles as a biomimetic delivery platform, Proc. Natl. Acad. Sci. U. S. A. 108 (2011) 10980–10985.

[30] K. Shinohara, T. Okita, M. Tsugane, T. Kondo, H. Suzuki, Sizing of giant unilamellar vesicles using a metal mesh with a high opening ratio, Chem. Phys. Lipids 241 (2021) 105148.

[31] C. Counil, E. Abenojar, R. Perera, A.A. Exner, Extrusion: a new method for rapid formulation of high-yield, monodisperse nanobubbles, Small 18 (2022) 2200810.

[32] A.W. Nafi, M. Taseidifar, R.M. Pashley, B.W. Ninham, The effect of amino acids on bubble coalescence in aqueous solution, J. Mol. Liq. 369 (2023) 120963.

[33] H.-A. Klok, J.J. Hwang, J.D. Hartgerink, S.I. Stupp, Self-assembling biomaterials: l-lysine-dendron-substituted cholesteryl-(l-lactic acid)n¯, Macromolecules 35 (2002) 6101–6111.

[34] C. Azevedo, A. Saiardi, Why always lysine? The ongoing tale of one of the most modified amino acids, Adv. Biol. Regul. 60 (2016) 144–150.

[35] H. Takahashi, T. Yasue, K. Ohki, I. Hatta, Structure and phase behaviour of dimyristoylphosphatidic acid/poly(L-lysine) systems, Mol. Membr. Biol. 13 (1996) 233–240.

[36] J. Zhu, H. An, M. Alheshibri, L. Liu, P.M.J. Terpstra, G. Liu, V.S.J. Craig, Cleaning with bulk nanobubbles, Langmuir 32 (2016) 11203–11211.

[37] M. Behari, A.M. Mohanty, D. Das, Influence of a plant-based surfactant on improving the stability of iron ore particles for dispersion and pipeline transportation, Powder Technol. 407 (2022) 117620.

[38] M. Behari, A. Mouli Mohanty, D. Das, Insights into the transport phenomena of iron ore particles by utilizing extracted Bio-surfactant from Acacia concinna (Willd.) Dc, J. Mol. Liq. 382 (2023) 121974.

[39] J.N. Meegoda, S. Aluthgun Hewage, J.H. Batagoda, Stability of nanobubbles, Environ. Eng. Sci. 35 (2018) 1216–1227.

[40] M. Niwano, T. Ma, K. Iwata, D. Tadaki, H. Yamamoto, Y. Kimura, A. Hirano-Iwata, Two-dimensional water-molecule-cluster layers at nanobubble interfaces, J. Colloid Interface Sci. 652 (2023) 1775–1783.

[41] L. Zandarashvili, A. Esadze, J. Iwahara, Chapter Two - NMR Studies on the Dynamics of Hydrogen Bonds and Ion Pairs Involving Lysine Side Chains of Proteins, in: C.Z. Christov (Ed.), Advances in Protein Chemistry and Structural Biology, Ed., Academic Press, 2013, pp. 37–80.

[42] O.N. Rogacheva, S.A. Izmailov, L.V. Slipchenko, N.R. Skrynnikov, A new structural arrangement in proteins involving lysine NH3+ group and carbonyl, Sci. Rep. 7 (2017) 16402.

[43] J.-Y. Kim, M.-G. Song, J.-D. Kim, Zeta potential of nanobubbles generated by ultrasonication in aqueous alkyl polyglycoside solutions, J. Colloid Interface Sci. 223 (2000) 285–291.

[44] T.T. Bui, D.C. Nguyen, M. Han, Average size and zeta potential of nanobubbles in different reagent solutions, J. Nanopart. Res. 21 (2019) 173.

[45] J. Su, A. Cavaco-Paulo, Effect of ultrasound on protein functionality, Ultrason. Sonochem. 76 (2021) 105653.